Proceedings of the 1999 IEEE
International Conference on Robotics & Automation
Detroit, Michigan • May 1999

Brachiation on a Ladder with Irregular Intervals

Jun Nakanishi† , Toshio Fukuda‡ and Daniel E. Koditschek*
† Dept. of Micro System Engineering, Nagoya University, Nagoya, Aichi 464-8603, Japan
‡ Center for Cooperative Research in Advanced Science and Technology, Nagoya University, Nagoya, Aichi 464-8603, Japan
* Dept. of Electrical Engineering and Computer Science, The University of Michigan, Ann Arbor, MI 48109-2110, USA

Abstract

We have previously developed a brachiation controller that allows a two degree of freedom robot to swing from handhold to handhold on a horizontal ladder with evenly space rungs as well as swing up from a suspended posture using a "target dynamics" controller. In this paper, we extend this class of algorithms to handle the much more natural problem of locomotion over irregularly spaced handholds. Numerical simulations and laboratory experiments illustrate the effectiveness of this generalization.

1 Introduction

This paper presents a control strategy for brachiation on a ladder with irregular intervals. Our interest in this problem arises from the general concern about how dynamically dexterous robotic tasks can be achieved by combining physical insight into the designated task and the intrinsic dynamics of the robot in its environment. The study of brachiation has design implications for other tasks involving dynamical dexterity such as legged locomotion, [8, 12], dexterous manipulation [1, 2, 4] and underactuated systems [15].

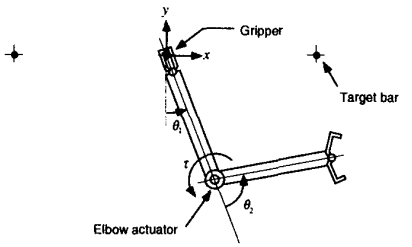

Figure 1: A two-link brachiating robot

For the last few years, we have been studying the control of the two degree of freedom brachiating robot depicted in Figure 1, which dynamically moves from handhold to handhold like a long armed ape. We initially proposed a new control algorithm based upon what we termed the "target dynamics" method. Motivated by the desire to have the robot's trajectories mimic the pendulous motion of an ape's brachiation, this method enabled us to force a one degree of freedom virtual composite of the physical 2 dof revolute-revolute kinematics to oscillate as if governed by the equations of motion of a harmonic oscillator [6]. Preliminary analysis, extensive simulation [6] and subsequent experimental studies [7] confirmed the proposed algorithm could achieve brachiation as well as swing up from a one hand to a two hand grip on a level ladder with uniform intervals.

*This work was supported in part by NSF IRI-9510673

The question remains whether this approach is likely to yield a flexible enough repertoire of behaviors to motivate its further analytical and experimental exploration. In this paper we take the modest step of increasing the behavioral repertoire to include the "irregular ladder problem" – brachiation on a ladder with irregularly spaced rungs placed at the same height. This addition seems to be essential, if only from the point of view of our initial biomechanics motivation, since very few unstructured environments confront an ape with equally spaced branches. The original robot brachiation studies by Saito *et al.* [3, 9, 10, 11] considered brachiation on bars with different distances and heights using heuristic learning and neural networks [10]. However, experimental implementation of their control algorithms were not carried out in the irregular ladder problem because of the enormous experimental burden and parametric iterations required of the physical robot[1]. Here, we employ a deadbeat style control strategy to solve the irregular ladder problem by extending the results in our previous studies. Numerical simulation and experimental results illustrate the effectiveness of our approach.

2 Experimental Setup[2]

2.1 Physical Apparatus

This section briefly describes our experimental system. We use the two-link brachiating robot originally developed by Saito [11] having updated the controller hardware (computer, input-output devices and motor driver circuits). Figure 2 depicts the experimental setup. The length of each arm is 0.5m and the total weight of the robot is about 4.8kg. The details of the description of the robot can be found in [7].

2.2 Model

The dynamical equations used to model the robot depicted in Figure 3 take the form of a standard two-link planar manipulator

$$\dot{Tq} = \mathcal{L}(Tq, v_r) \tag{1}$$

where

$$\mathcal{L}(Tq, v_r) = \begin{bmatrix} \dot{q} \\ M^{-1}\left(-V - k - B\dot{q} - C\mathrm{sgn}(\dot{q}) + \begin{bmatrix} 0 \\ Kv_r \end{bmatrix}\right) \end{bmatrix},$$

$q = [\,\theta_1,\ \theta_2\,]^T \in \mathcal{Q}$, $Tq = [\,q^T,\ \dot{q}^T\,]^T \in T\mathcal{Q}$, M is the inertia matrix, V is the Coriolis/centrifugal vector, and k is the gravity vector. C and B denote the coulomb and viscous friction coefficient matrices respectively. We assume

[1] They did implement the learning algorithm on the physical two-link robot in the uniform ladder problem [11].

[2] Portions of this section are excerpted from [7].

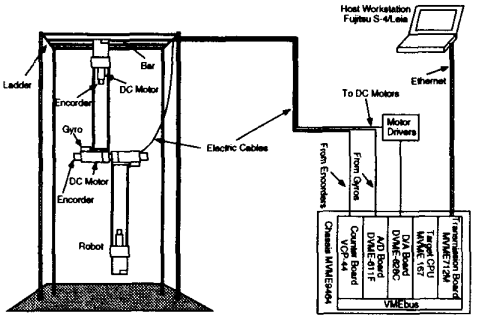

Figure 2: The experimental setup of the two-link brachiating robot.

that the elbow actuator produces torque proportional to a voltage command, v_r, sent to a driver as $\tau = Kv_r$, where K is a positive constant. It is generally known that DC

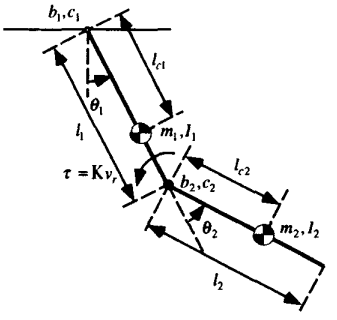

Figure 3: The mathematical model of the two-link brachiating robot used in this paper.

motors with harmonic gear mechanisms bear complicated nonlinear characteristics [16]. However, for simplicity, we model the dynamics of the elbow actuator using only viscous and coulomb friction and rotor inertia. As the results of parameter identification presented in [7] suggest, the model we offer here fits the dynamics of the physical system fairly well. The dynamical parameters of the robot are shown in Table 1.

Description		i=1	i=2
Mass	m_i(kg)	3.499	1.232
Moment of inertia	I_i(kgm^2)	0.090	0.033
Link length	l_i(m)	0.50	0.50
Location of CG	l_{ci}(m)	0.414	0.333
Viscous friction	b_i(Nm/s)	0.02	0.14
Coulomb friction	c_i(Nm)	0.02	0.45
Torque constant	K(Nm/V)	1.752	

Table 1: The dynamical parameters of the robot obtained by the procedure described in [7].

3 Irregular Ladder Problem[3]

In this section, we present our control strategy for brachiation on a ladder with irregular intervals. First, we review our "target dynamics" strategy and its application to the uniform ladder problem and the rope problem discussed in [6]. Next, we introduce a deadbeat style strategy which extends these ideas to the present problem setting.

3.1 Review of the Uniform Ladder Controller

A detailed development of the target dynamics controller can be found in [6]. The strategy is a particular instance of input/output linearization Specifically, brachiation is encoded as the output of a target dynamical system—a harmonic oscillator determined by a "virtual frequency", ω, which we will force the robot to mimic. At the end of [6], we define the controller for the lossless model where $B, C \to 0$

$$\begin{aligned}\tau &:= \left(D_q h \begin{bmatrix} n_{12} \\ n_{22} \end{bmatrix}\right)^{-1} \left[-\omega^2\theta - (\dot{D_q h})\dot{q} + D_q h M^{-1}(V+k)\right] \\ &= \frac{1}{n_{12}+\frac{1}{2}n_{22}} \left[-\omega^2(\theta_1+\frac{1}{2}\theta_2) + (n_{11}+\frac{1}{2}n_{21})(V_1+k_1)\right] \\ &\quad + V_2 + k_2 \end{aligned} \tag{2}$$

where, $h(q) := \theta = \theta_1 + \frac{1}{2}\theta_2$, n_{ij} denotes each component of M^{-1}, and $v_r = \frac{1}{K}\tau$. In the subsequent simulations and experiments, we use the lossy model, and the friction terms are added in the controller to cancel them. Note that

$$D_q h \begin{bmatrix} n_{12} \\ n_{22} \end{bmatrix} = \frac{m_1 l_{c1}^2 + m_2(l_1^2 - l_{c2}^2) + I_1 - I_2}{2\det(M)} \neq 0, \tag{3}$$

i.e., the invertibility condition of the first term in (2) is satisfied in the particular setting of concern.

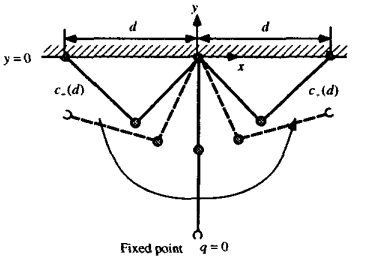

Figure 4: The ceiling is parametrized by the distance between the grippers d. A left branch $c_-(d)$ and right branch $c_+(d)$ are defined in this manner.

The ladder problem arises when an ape transfers from one branch to another and the control of arm position at the next capture represents the control task requirement. Here, we restrict our attention to brachiation on a set of evenly spaced bars at the same height. We showed in [6] how a symmetry property of an appropriately chosen target system — determined by ω in (2) — can solve this problem. The next question concerns the choice of ω in the target dynamics to achieve the desired motion. This is determined according to the principle of "neutral orbits" defined in [6, 13, 14]. Namely, following Raibert [8], a "neutral orbit" is one with a reverse time symmetry whereby orbits forward in time from the bottom are horizontal reflections of orbits backward in time from the same bottom state[4]. In the sequel, we will denote the integral curve of a vector field f by the notation f^t.

Define the "ceiling" to be those configurations where the hand of the robot reaches the height $y = 0$ as depicted

[3] Portions of sections 3.1 and 3.2 are excerpted from [6].

[4] The "bottom states" are those characterized by both joint angles at zero: i.e. the arm is hanging straight down.

in Figure 4,

$$\mathcal{C} = \{q \in Q | \cos\theta_1 + \cos(\theta_1 + \theta_2) = 0\}. \quad (4)$$

Note that $\mathcal{C}$ can be parameterized by two branches,

$$\mathcal{C} = \text{Im } c_- \cup \text{Im } c_+ \quad (5)$$

of the maps

$$c_\pm(d) = \begin{bmatrix} \pm \arcsin\left(\frac{d}{2l}\right) \\ \pm\left[\pi - 2\arcsin\left(\frac{d}{2l}\right)\right] \end{bmatrix}, \quad (6)$$

where $l = l_1 = l_2$. Suppose we have chosen a feedback law, $\tau(q, \dot{q})$, denote the closed loop dynamics of the robot as

$$\dot{T}q = \mathcal{L}_\tau(q, \dot{q}) = \mathcal{L}(Tq, \tau(q, \dot{q})). \quad (7)$$

In the sequel, we will be particularly interested in initial conditions of (7) originating in the zero velocity sections of the ceiling that we denote TC_0 in (13). We conclude in [6] that any feedback law, τ, which respects the reverse time symmetry solves the ladder problem, assuming we can find d such that $[\, c_-(d)^T,\ 0,\ 0\,]^T$ is in a neutral orbit. Note that finding such a ceiling point requires solving the equation

$$\Phi(d, t_N) = [\ I\ ,\ \ 0\ ]\,\mathcal{L}_\tau^\nu\left(\begin{bmatrix} c_-(d) \\ 0 \\ 0 \end{bmatrix}\right) = \begin{bmatrix} 0 \\ 0 \end{bmatrix}, \quad (8)$$

for d and t_N simultaneously, where $\nu = \frac{t_N}{4}$ and I is a 2×2 identity matrix. Of course solving this equation is very difficult: it requires a "root finding" procedure that entails integrating the dynamics, $\mathcal{L}$.

The feedback law to achieve the desired target dynamics is given by (2). We show in [6] that the choice of the target dynamical system – a harmonic oscillator — has a very nice property relative to the difficult root finding problem (8). Namely, using this control algorithm, t_N is given by

$$t_N(\tau_\omega) = \frac{2\pi}{\omega} \quad (9)$$

because θ follows the target dynamics $\ddot{\theta} = -\omega^2\theta$. In this light, then, we need merely solve (8) for d. More formally, we seek an implicit function $d^* = \lambda^{-1}(\omega)$ such that $\Phi\left(\lambda^{-1}(\omega), \frac{2\pi}{\omega}\right) = 0$. In practice, we are more likely to take an interest in tuning ω as a function of a desired distance between the bars, d^*. Thus, we are most interested in determining

$$\omega = \lambda(d^*). \quad (10)$$

In general, we can expect no closed form expression for λ or λ^{-1}, and we resort instead to a numerical procedure for determining an estimate, $\hat{\lambda}$. The details of the numerical procedure is discussed in [5]. In Figure 5 we plot a particular instance of $\hat{\lambda}$ for the case where the robot parameters are as specified in Table 1.

3.2 Rope Problem: Review

In this section, we consider the rope problem discussed in [6]: brachiation along a continuum of handholds such as afforded by a branch or a rope. First, the average horizontal velocity is characterized as a result of the application of the target dynamics controller, τ_ω, introduced above. Then, we consider the regulation of horizontal velocity using this controller. An associated numerical "swing map"

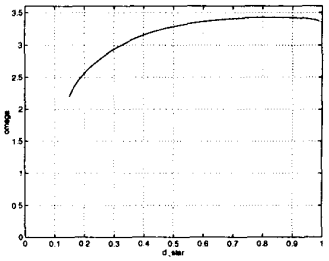

Figure 5: Numerical approximation $\omega = \hat{\lambda}(d^*)$. Target dynamics controller, τ_ω, is tuned according to this mapping, $\hat{\lambda}$, that is designed to locate neutral orbits originating in the ceiling.

suggests that we indeed can achieve good local regulation of the foward velocity through the target dynamics method.

Supposing that the robot starts in the ceiling with zero velocity, then it must end in the ceiling under the target dynamics controller since θ follows the target dynamics $\ddot{\theta} = -\omega^2\theta$. However, if d and ω are not "matched" as $\omega = \lambda(d)$, then the trajectory ends in the ceiling, $Tq \in TC_+$, with $\dot{\theta} = 0$ but $r \neq d$ and $\dot{r} \neq 0$. Here, (r, θ) denots the position of the gripper in polar coordinates arising from the change of coordinates from joint space. This leads to the definition of the swing map.

When a gripper moves a distance $2d^*$ in the course of the ladder trajectory, and if the trajectory is immediately repeated, then the body will also move a distance of d^* each swing, hence, its average horizontal velocity will be

$$\bar{\dot{h}} = \frac{d^*\omega}{\pi} = \frac{d^*\lambda(d^*)}{\pi} := \tilde{V}(d^*) \quad (11)$$

according to the previous discussion.

Consider now the task of obtaining the desired forward velocity $\bar{\dot{h}}^*$ of brachiation. If $\tilde{V}$ is invertible, then $d^* = \tilde{V}^{-1}(\bar{\dot{h}}^*)$ and we can tune ω in the target dynamics as

$$\omega = \lambda \circ \tilde{V}^{-1}(\bar{\dot{h}}^*) \quad (12)$$

to achieve a desired $\bar{\dot{h}}^*$ where λ is again the mapping (10). Consider the ceiling condition with zero velocity

$$TC_{0\pm} = \{[\, c_\pm(d)^T,\ 0,\ 0\,]^T \in TC \mid d \in [0, 2l]\} \quad (13)$$

Define the maps, $C_\pm$, relating d and the initial state of the robot, and Π which "kills" any velocity in the ceiling as

$$C_\pm : [0, 2l] \to TC_{0\pm} : d \mapsto [\, c_\pm(d)^T,\ 0,\ 0\,]^T \quad (14)$$

$$\Pi : TC_\pm \mapsto TC_{0\pm}. \quad (15)$$

We now define a "swing map" [6], σ_ω, as a transformation of $[0, 2l]$ into itself,

$$\sigma_\omega(d) := C_+^{-1} \circ \Pi \circ \mathcal{L}_{\tau_\omega}^{2\nu} \circ C_-(d) : [0, 2l] \to [0, 2l] \quad (16)$$

Note that if $\omega = \omega^* = \lambda(d^*)$, then

$$\sigma_\omega(d^*) = d^* \quad (17)$$

that is, d^* is a fixed point of the appropriately tuned swing map. Suppose we iterate by setting the next initial condition in the ceiling to be

$$Tq_0[k+1] = C_- \circ \sigma_\omega(d[k]). \tag{18}$$

This yields a discrete dynamical system governed by the iterates of σ_ω,

$$d[k+1] = \sigma_\omega(d[k]). \tag{19}$$

Numerical evidence suggests that the iterated dynamics converges, $\lim_{k\to\infty} \sigma^k_{\omega^*}(d) = d^*$ when d is in the neighborhood of d^* [6].

3.3 Deadbeat Control Strategy for Irregular Ladder Problem

This section presents a deadbeat style control strategy for the irregular ladder problem which extends the ideas discussed in the previous sections. Now, we consider brachiation on a ladder with irregularly spaced rungs placed at the same height as depicted in Figure 6. Using the target dynamics, a single parameter, ω, in the controller characterizes the full range of the swing motion of the robot. Now, we seek the tuning rule for ω which locates the desired orbit from $C_-(d[k])$ to $C_+(d[k+1])$.

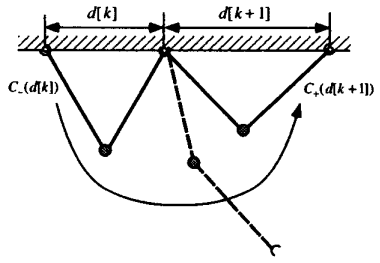

Figure 6: The irregular ladder problem. The robot moves from the left branch to the right branch with the intervals $d[k]$ and $d[k+1]$.

Define a new function

$$\tilde{\lambda} : [0, 2l] \times [0, 2l] \to I\!R \tag{20}$$

to solve the implicit function in ω by (19):

$$\tilde{\lambda}(d_1, d_2) := \text{solve}_{\omega \in I\!R}[d_2 - \sigma_\omega(d_1) = 0], \tag{21}$$

where d_1 and d_2 are the intervals between the bars of the left branch and the right branch respectively. This function is computed numerically and involves integrating the Lagrangian dynamics as in (18). In practice, we find that $\tilde{\lambda}$ is well defined only on a subset $\mathcal{D} \subseteq [0, 2l]$ whose extent depends upon the dynamical parameters of the robot as

$$\omega = \tilde{\lambda}(d[k], d[k+1]) : \mathcal{D} \times \mathcal{D} \to I\!R, \tag{22}$$

where $\mathcal{D} \subseteq [0, 2l]$. We plot in Figure 7 a particular instance of $\tilde{\lambda}$ for the case where the robot parameters are as specified in Table 1. The target dynamics controller is tuned according to this mapping to locate the orbit which achieves the desired gait of locomotion. Note that the mapping, $\omega = \lambda(d^*)$, in (10) is the intersection of the surface, $\tilde{\lambda}$, and the plane $d[k] - d[k+1] = 0$.

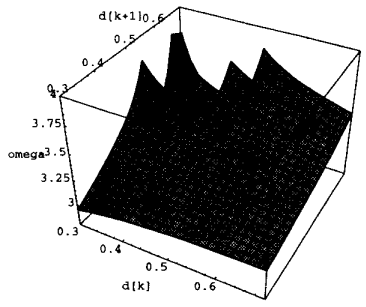

Figure 7: Numerical approximation of $\omega = \tilde{\lambda}(d[k], d[k+1])$. Target dynamics controller, τ_ω, is tuned according to this mapping, $\tilde{\lambda}$, that is designed to locate the desired orbit.

4 Simulation

Consider the following three cases of the intervals between the bars as specified in Table 2. The initial condition of the robot is $Tq_0 = [c_-(d[k])^T, 0, 0]$. From the numerical solution to the mapping (22) depicted in Figure 7, ω is tuned for each case as shown in Table 2.

Case	$d[k]$	$d[k+1]$	ω
1	0.4	0.6	3.66
2	0.5	0.6	3.47
3	0.6	0.5	3.255

Table 2: Intervals between the bars and ω considered in numerical simulation and experiments.

In this simulation, we use the lossy model with the dynamical parameter as specified in Table 1. Note that discontinuity of the voltage command observed in Figures 9 and 11 results from the coulomb friction terms added in the controller. These simulation results suggest the effectiveness of the proposed strategy.

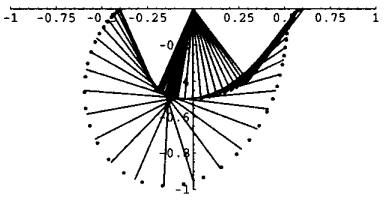

Figure 8: Movement of the robot (simulation), where $d[k] = 0.4, d[k+1] = 0.6$.

Case 1: $d[k] = 0.4, d[k+1] = 0.6$ Figure 8 depicts the movement of the robot, and Figure 9 shows the joint trajectories and the voltage command to the motor driver.

Case 2: $d[k] = 0.5, d[k+1] = 0.6$ Figure 10 depicts the movement of the robot, and Figure 11 shows the joint trajectories and the voltage command to the motor driver.

Case 3: $d[k] = 0.6, d[k+1] = 0.5$ Figure 12 depicts the movement of the robot, and Figure 13 shows the joint trajectories and the voltage command to the motor driver.

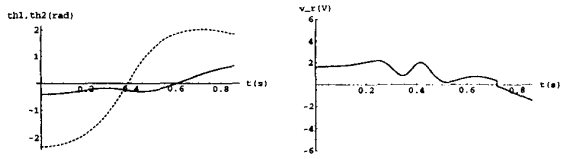

Figure 9: The simulation results, where $d[k] = 0.4, d[k+1] = 0.6$. Left: Joint trajectories (solid: θ_1, dashed: θ_2) , Right: Voltage command to the motor driver.

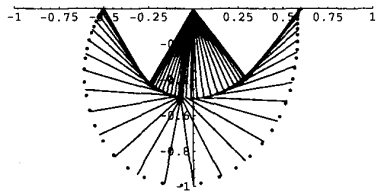

Figure 10: Movement of the robot (simulation), where $d[k] = 0.5, d[k+1] = 0.6$.

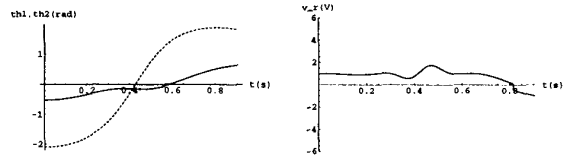

Figure 11: The simulation results, where $d[k] = 0.5, d[k+1] = 0.6$. Left: Joint trajectories, (solid: θ_1, dashed: θ_2), Right: Voltage command to the motor driver.

5 Experiments

This section presents the experimental implementaion of the proposed control strategy. We consider the same ladder intervals as specified in Table 2.

As we have experienced in our previous experimental work [7], we refine the dynamical parameters in the controller and the timing of bar release manually so that the robot successfully achieves the desired brachiation because of the parameter mismatch and a delay in the actuator mechanism the gripper. The command to close the gripper is sent and the voltage command to the motor driver is turned off simultaneously when the gripper approaches the target bar. Some experience is helpful in these refinements.

Case 1: $d[k] = 0.4, d[k+1] = 0.6$ The typical movement of the robot is depicted in Figure 14, while the joint trajectories and the voltage commands sent to the driver are shown in Figure 15. We choose to use the dynamical parameters, $m_1 = 3.39, m_2 = 1.30, c_2 = 0.65, b_2 = 0.9$, instead of the values shown in Table 1. The mean time of ten runs at which the robot reaches the ceiling is 0.949 seconds with ± 0.04 second error, which is close to its analytical value, $t = \frac{\pi}{\omega} = 0.854$ seconds.

Case 2: $d[k] = 0.5, d[k+1] = 0.6$ The typical movement of the robot is depicted in Figure 16, while the joint trajectories and the voltage commands sent to the driver are shown in Figure 17. We choose to use the dynamical parameters, $m_1 = 3.39, m_2 = 1.30, c_2 = 0.73, d_2 = 0.6$, instead of the values shown in Table 1 and send the command to open the gripper 0.01 seconds before the controller is turned on. The mean locomotion time of ten runs is 0.870 seconds with ± 0.03 second error, which is close to its analytically calculated value, $t = \frac{\pi}{\omega} = 0.905$ seconds.

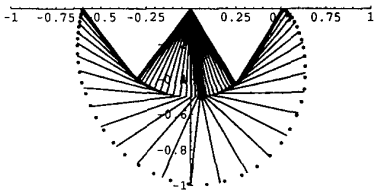

Figure 12: Movement of the robot (simulation), where $d[k] = 0.6, d[k+1] = 0.5$.

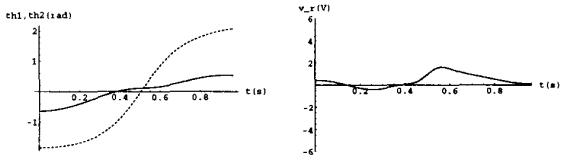

Figure 13: The simulation results, where $d[k] = 0.6, d[k+1] = 0.5$. Left: Joint trajectories, (solid: θ_1, dashed: θ_2), Right: Voltage command to the motor driver.

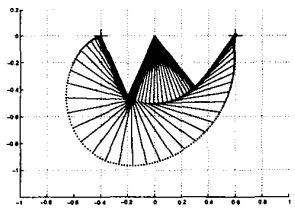

Figure 14: Movement of the robot (experiment), where $d[k] = 0.4, d[k+1] = 0.6$.

Case 3: $d[k] = 0.6, d[k+1] = 0.5$ The typical movement of the robot is depicted in Figure 18, while the joint trajectories and the voltage commands sent to the driver are shown in Figure 19. We choose to use the dynamical parameters, $m_1 = 3.39, m_2 = 1.30, c_2 = 0.73, b_2 = 0.33$, instead of the values shown in Table 1 and send the command to open the gripper 0.08 seconds before the controller is turned on. The mean locomotion time of ten runs is 0.841 seconds with ± 0.08 second error, which is very close to its analytical value, $t = \frac{\pi}{\omega} = 0.965$ seconds.

As we have begun to investigate the discrepancy between the simulation and experiments seen above, numerical studies suggest that this seems to be due to the model mismatch of the friction and unmodelled torque saturation of the elbow actuator.

6 Conclusion

We present a deadbeat style control strategy which increases the behavioral repertoire of a brachiating robot to handle irregularly space handholds by an appropriate modification of our earlier "target dynamics controller." Numerical simulation and experimental results illustrate the effectiveness of this strategy. More analytical work will be required to completely understand the effect of this

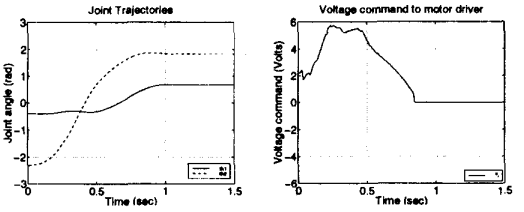

Figure 15: The experimental results, where $d[k] = 0.4, d[k+1] = 0.6$. Left: Joint trajectories (solid: θ_1, dashed: θ_2) , Right: Voltage command to the motor driver.

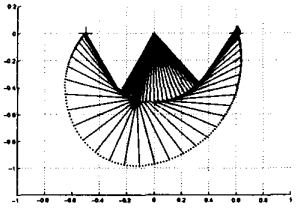

Figure 16: Movement of the robot (experiment), where $d[k] = 0.5, d[k+1] = 0.6$.

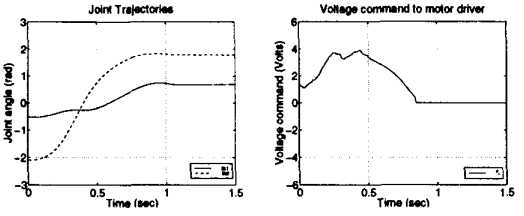

Figure 17: The experimental results, where $d[k] = 0.5, d[k+1] = 0.6$. Left: Joint trajectories (solid: θ_1, dashed: θ_2) , Right: Voltage command to the motor driver.

style of controller on such underactuated mechanisms.

Motivated by the close analogy between brachiation and legged locomotion, future directions of work in this area suggest the desirability of "passive" or somewhat less model dependent approaches. In the more distant future, we are interested as well in "leaping" gaits analogous to an ape's fast brachiation that include a nonholonomic flight phase. We are hopeful that the ideas presented here may still have wider applications to other problems in the study of dynamical dexterous robotics.

References

[1] Andersson, R. L. *A Robot Ping-Pong Player: Experiment in Real-Time Intellgent Control.* MIT Press, 1988.

[2] Bühler, M., Koditschek, D. E., and Kindlmann, P. J. Planning and control of robotic juggling and catching tasks. *International Journal of Robotics Research*, 13(2):101–118, April 1994.

[3] Fukuda, T., Saito, F., and Arai, F. A study on the brachiation type of mobile robot (heuristic creation of driving input and control using CMAC. In *IEEE/RSJ International Workshop on Intelligent Robots and Systems*, pages 478–483, 1991.

[4] Lynch, K. M. *Nonprehensile Robotic Manipulation: Controllability and Planning.* PhD thesis, Carnegie Mellon University, The Robotics Institute, March 1996.

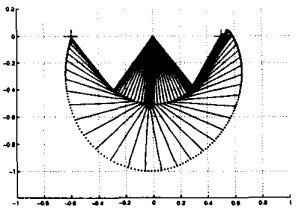

Figure 18: Movement of the robot (experiment), where $d[k] = 0.6, d[k+1] = 0.5$.

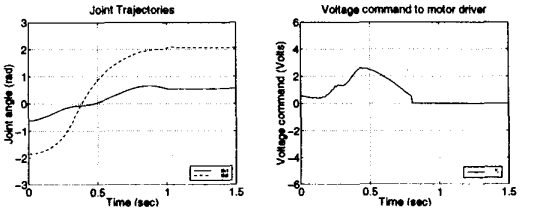

Figure 19: The experimental results, where $d[k] = 0.6, d[k+1] = 0.5$. Left: Joint trajectories (solid: θ_1, dashed: θ_2) , Right: Voltage command to the motor driver.

[5] Nakanishi, J., Fukuda, T., and Koditschek, D. E. Preliminary analytical approach to a brachiation robot controller. Technical report: CGR 96-08 / CSE TR 305-96, The Univ. of Michigan, EECS Depertment, August 1996.

[6] Nakanishi, J., Fukuda, T., and Koditschek, D. E. Preliminary studies of a second generation brachiation robot controller. In *IEEE International Conference on Robotics and Automation*, pages 2050–2056, April 1997.

[7] Nakanishi, J., Fukuda, T., and Koditschek, D. E. Experimental implementation of a "target dynamics controller on a two-link brachiating robot". In *IEEE International Conference on Robotics and Automation*, pages 787–792, May 1998.

[8] Raibert, M. H. *Legged Robots that Balance.* MIT Press, 1986.

[9] Saito, F. *Motion Control of the Brachiation Type of Mobile Robot.* PhD thesis, Nagoya University, March 1995. (in Japanese).

[10] Saito, F., Fukuda, T., and Arai, F. Movement control of brachiation robot using CMAC between different distance and height. In *IMACS/SICE International Symposium on Robotics, Mechatronics and Manufacturing Systems*, pages 35–40, 1992.

[11] Saito, F., Fukuda, T., and Arai, F. Swing and locomotion control for a two-link brachiation robot. *IEEE Control Systems Magazine*, 14(1):5–12, February 1994.

[12] Schwind, W. J. *Spring Loaded Inverted Pendulum Running: A Plant Model.* PhD thesis, The University of Michigan, Dept. of EECS, September 1998.

[13] Schwind, W. J. and Koditschek, D. E. Control the forward velocity of the simplified planner hopping robot. In *IEEE International Conference on Robotics and Automation*, pages 691–696, 1995.

[14] Schwind, W. J. and Koditschek, D. E. Characterization of monoped equilibrium gaits. In *IEEE International Conference on Robotics and Automation*, pages 1986–1992, 1997.

[15] Spong, M. The swing up control problem for the acrobot. *IEEE Control Systems Magazine*, 15(1):49–55, February 1995.

[16] Tuttle, T. D. and Seering, W. P. A nonlicar model of a harmonic drive gear transmission. *IEEE Transaction on Robotics and Automation*, 12(3):368–374, June 1996.